Damghan University Press

Journal of Nano Simulation
journal homepage: jons.du.ac.ir

Volume 2, Issue 1, Winter 2026, 36-46
DOI: 10.22128/jons.2025.1042.1011

Quantum mechanical study of the interaction of letrozole with PLGA nanoparticles as drug carriers

Laleh Khorshidi[*,1], Davood Farmanzadeh [1], Sima Esmailpour [2]

[1.] *Department of Physical Chemistry, Faculty of Chemistry, University of Mazandaran, Babolsar, Iran*
[2.] *Faculty of Chemistry, Shahrood University of Technology, Shahrood, Iran*

HIGHLIGHTS

- This article examines the quantum interaction of letrozole (LET), an anticancer drug, with PLGA monomers used as drug carriers.
- DFT calculations at B3LYP/6-31G(d,p) level analyze structural, thermodynamic, and electronic properties of covalent and non-covalent interactions.
- Adding ethylene glycol (EG) and optimizing monomer positions significantly lowers the adsorption energy and HOMO-LUMO gap.
- This reduction enhances the complexes' reactivity and thermodynamic stability.
- Results highlight PLGA's potential for targeted letrozole delivery in cancer therapy.

GRAPHICAL ABSTRACT

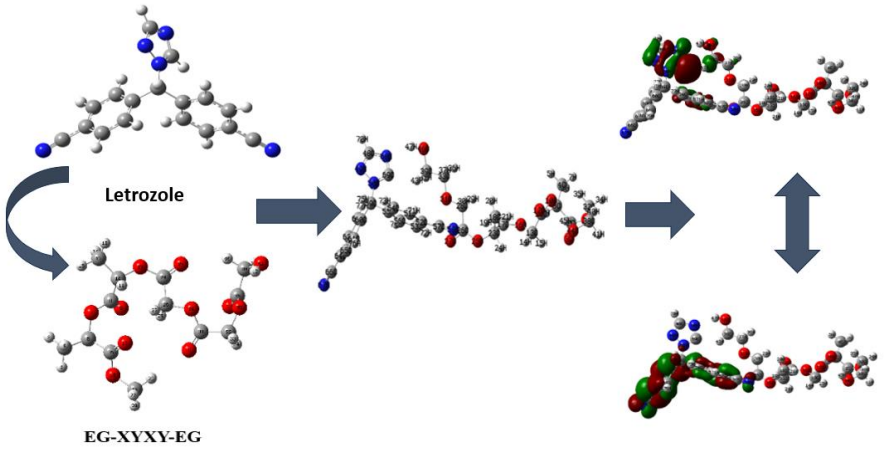

ARTICLE INFO

Article history:
Received: 2025-07-01
Received in revised form: 2025-09-17
Accepted 2026-01-20

Available online:2026-02-26

Keywords:
Letrozole, anticancer,
PLGA (poly(lactic-co-glycolic) acid),
drug delivery,
Monomers,
Density Functional Theory

ABSTRACT

Letrozoles are a group of organic compounds that have anticancer properties in gynecological diseases, including breast and ovarian cancer. The drug acts by inhibiting the aromatase enzyme, reducing estrogen levels, and thereby reducing tumor growth. Considerable efforts have also been made in developing new methods for precisely delivering drugs to specific target sites. As a result, there is a pressing need to administer precise doses of drugs directly to the desired site for an appropriate period of time. PLGA (poly(lactic-co-glycolic) acid) is a biodegradable copolymer commonly used in drug delivery. This copolymer is composed of X and Y monomers, which affect its physical and chemical properties. Using density functional theory (DFT) calculations, the structural, electronic, and thermodynamic properties of the interaction of LET with PLGA monomers were investigated. The interaction of letrozole with PLGA monomers was investigated in two covalent and non-covalent states. The results showed that the degree of interaction depends on the number of monomers and their position, the attachment or not of ethylene glycol, and the site of drug attachment to the structures, such that in some cases the covalent interaction is more significant and in some other cases the non-covalent interaction is more significant

* Corresponding author: E-mail address: laleh_khorshidi@yahoo.com

Introduction

Letrozole (LET) is an organic compound containing a nitrile group, consisting of two six-membered rings and one five-membered ring with three nitrogen atoms replacing carbons. It has gained attention for its medicinal properties, particularly its anticancer effects in breast and ovarian cancers [1, 2]. Approved by the FDA for breast cancer chemotherapy, LET inhibits the aromatase enzyme, lowers estrogen levels, and reduces tumor growth. It is a selective non-steroidal inhibitor used in advanced breast and uterine cancers. Molecular studies indicate that LET can undergo two metabolic pathways, producing either an inactive metabolite with a large HOMO-LUMO gap or a more reactive one with a smaller gap [3]. Considering that the anticancer drug LET contains two cyanide groups attached to a six-membered ring and three nitrogen atoms within the five-membered ring, an initial investigation was conducted into the nitrogen atoms of the cyanide groups present in this drug. Subsequently, the focus was directed to the nitrogen atoms within the five-membered ring [4]. Significant efforts have been made not only in designing anticancer agents but also in developing novel methods for precisely delivering drugs to specific target sites. While treatments such as chemotherapy, radiation therapy, and immunotherapy remain the main approaches for fighting aggressive cancers, a major challenge is the lack of selectivity exhibited by many anticancer drugs. This non-specific action can damage healthy cells and cause toxic side effects, even at higher doses [5]. Therefore, there is a critical need to deliver the exact dose of the drug directly to the target site for an appropriate duration. Achieving targeted and efficient drug delivery is a complex task, prompting ongoing research into the development of specialized carriers to improve this process [6]. Owing to their customizable properties, poly-lactic-co-glycolic acid (PLGA) microparticles are increasingly gaining importance in the field of nanomedicine [7]. In recent years, many synthetic polymers, especially PLGA, have been investigated as drug delivery systems in nanomedicine. PLGA is notable for its biodegradability, ability to form nanometric micelles, and controlled drug release, making it a promising material for advanced drug carriers [8]. PLGA nanoparticles are among the most commonly used polymers in biomedicine due to their excellent biocompatibility and mechanical stability, making them suitable for medical applications such as sutures and fibers [9]. Their main advantage is their ability to self-assemble into structures like microcapsules and nanoparticles, suitable for drug delivery. These water-soluble systems can be administered locally or orally and loaded with various therapeutics for sustained release [10]. Additionally, understanding the interactions within biological systems is crucial for designing new therapeutic agents [11].Earlier, it was noted that PLGA is made up of monomers X and Y, which differ in their atomic composition and structure. These monomers can be arranged in different configurations and may undergo substitutions. Altering the quantity of monomers in the copolymer yields new polymers with distinct physical and chemical properties, resulting in variations in their structures and energy profiles [12]. In 2008, Ghahremankhani and colleagues investigated the use of a triblock copolymer comprised of PLGA – PEG – PLGA as a drug delivery system for transporting calcitonin [13]. In 2011, Makadia and Siegel demonstrated that PLGA is a biodegradable and biocompatible carrier suitable for the controlled delivery of small molecules, proteins, and macromolecules. Its long degradation time

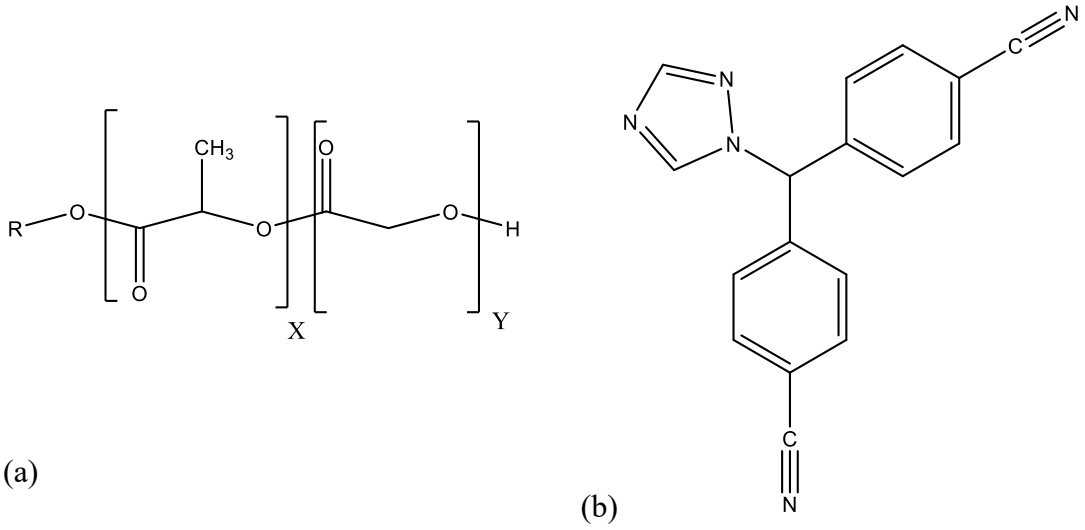

Figure 1 the structures of (a) polylactic-co-glycolic acid (PLGA) and (b) Letrozole (LET).

and tunable properties make it ideal for medical applications. Due to its stability and compatibility with nucleic acids, PLGA is a promising drug delivery vehicle. [14]. In 2014, Akçay and Bayrak conducted computational studies on anastrozole and LET to investigate the effects of chemotherapeutic drugs in breast cancer [15]. The structures of poly (lactic-co-glycolic acid) (PLGA) and the drug LET are shown in Figure 1.

This study investigates the interactions between LET and PLGA, focusing on interaction energies, optimal drug placement, and the effect of monomer substitution. As the first quantum-level analysis of this system, it aims to provide insights into drug–carrier mechanisms and support the development of improved drug delivery systems.

2. Computational details

In this study, all geometric optimizations of the molecules were carried out at the B3LYP/6-31G(d,p) level of theory [16]. The drug molecule was positioned in multiple orientations relative to the PLGA monomers, and the resulting geometries were optimized. Vibrational frequency calculations were performed at the same level to confirm the nature of the optimized structures. No imaginary frequencies were observed, and all computed vibrational frequencies were positive, indicating that the optimized structures correspond to true minima on the potential energy surface (data not shown) .After optimizing all configurations resulting from the interaction of the LET drug with various states of PLGA monomers, the adsorption energies were initially calculated based on Eq 1.

$$E_{Ads} = E_{Complex} - (E_{LET} + E_{PLGA\ monomers}) \quad (1)$$

In this context, E_{ads} represents the adsorption energy of the drug molecule and its complexes in the respective configuration, where E_{PLGA} corresponds to the energy of PLGA monomers, E_{LET} pertains to the energy of the drug, and $E_{Complex}$ denotes the energy of the drug–PLGA monomer complex.

To obtain a more quantitative assessment of the complexes' stability, the thermodynamic parameters, specifically the changes in Gibbs free energy (ΔG) and enthalpy (ΔH), were computed using frequency analysis [17]. The following equation expresses these thermodynamic variations:

$$\Delta M = M_{Complex} - (M_{LET} + M_{PLGA\ monomers}) \quad (2)$$

where ΔM represents the quantity of ΔG and ΔH. Furthermore, $M_{LET\cdots PLGA\ monomers}$, M_{LET}, and $M_{PLGA\ monomers}$ introduce the G/H parameters of the optimized complexes, the LET drug, and PLGA monomers nanocarriers, respectively.

To explore the electronic characteristics, the frontier molecular orbital (FMO) theory was employed. In this approach, the electron density distributions of the highest occupied molecular orbital (HOMO) and the lowest unoccupied molecular orbital (LUMO) were visualized both prior to and following adsorption. Additionally, the energies associated with HOMO (E_{HOMO}) and LUMO (E_{LUMO}) were determined. Using these values, the Fermi level (E_F) and the energy gap between LUMO and HOMO (E_{gap}) were calculated through Equations (3) and (4), respectively.

$$E_F = E_{HOMO} + \frac{E_{gap}}{2} = \frac{E_{HOMO} + E_{LUMO}}{2} \quad (3)$$

$$E_{gap} = E_{LUMO} - E_{HOMO} \quad (4)$$

Different electronic characteristics such as ionization energy (IP), electron affinity (EA), chemical potential (μ), global hardness (η), global softness (S), electrophilicity index (ω), and work function (Φ) were evaluated for the LET molecule and its complex before and following adsorption, as detailed below [18, 19]:

$$IP = -E_{HOMO} \quad (5)$$

$$EA = -E_{LUMO} \quad (6)$$

$$\mu = \frac{(E_{HOMO} + E_{LUMO})}{2} \quad (7)$$

$$\eta = \frac{(E_{LUMO} - E_{HOMO})}{2} \quad (8)$$

$$S = \frac{1}{2\eta} \quad (9)$$

$$\omega = \frac{\mu^2}{2\eta} \quad (10)$$

$$\Phi = V_{el}(+\infty) - E_F \quad (11)$$

The vacuum-level electrostatic potential, denoted as $V_{eL}(+\infty)$, is considered to be approximately zero [20]. All density functional theory (DFT) computations were performed using the Gaussian 09 software [21], employing the B3LYP functional in conjunction with the 6-31G (d,p) basis set.

3. Results and discussion

3.1. Geometric optimization of the structures

Given the crucial role of PLGA monomers in drug delivery systems, this section investigates the interaction between the drug LET and select PLGA monomers. The outcomes of these computational analyses are intended to inform the design of novel drug carriers and therapeutic compounds. When identifying optimal interaction sites

between LET and PLGA monomers, the molecular structure of LET must be carefully considered. Based on its structural features (Figure 1), the rings attached to the nitrile group and the five-membered triazole ring are deemed suitable for interaction studies with PLGA molecules. Accordingly, these sites were selected for detailed analysis. By positioning LET at an appropriate distance from the PLGA monomers, geometry optimizations and frequency calculations were subsequently performed to characterize the stability and nature of the complexes. Initial optimization of each PLGA monomer–LET complex was carried out at the B3LYP/6-31G(d,p) level of theory. The optimized structures of these complexes are presented in Figure 2.

An analysis of the optimized geometries indicates that the interaction of LET with various PLGA monomers induces changes in bond lengths and angles, contingent upon the specific interaction site. Figure 2(a) illustrates the optimized geometry of the LET-XXXY complex, where the triazole ring of LET approaches the PLGA molecule. Notably, the distance between O65 and C22 decreases from 2.59 Å in the initial structure to 1.34 Å post-optimization, consistent with bond formation. Further analysis of the structure in Figure 2(b) reveals that in the optimized LET-XXYX complex, the O66–C22 distance reduces from 2.79 Å to 1.33 Å upon complexation. Similarly, in the LET-XYXX complex (Figure 2(c)), this distance decreases from 3.04 Å to 1.36 Å, indicating comparable interaction patterns. Figures 2(d) and e depict the optimized geometries of the LET-XY and LET-EG-XY-EG complexes, respectively. In the d complex, as the triazole ring approaches the glycolic acid segment (Y), the distance between N24 and H19 decreases markedly from 4.14 Å to 1.89 Å, suggesting the formation of a stable interaction. Conversely, in the E complex, the proximity of the six-membered nitrile-containing ring results in an increased equilibrium distance between O56 and C19 from 2.36 Å to 3.96 Å, implying that LET interacts effectively with the EG moiety of the EG-XY-EG molecule via its nitrile group on the ring. A comprehensive analysis of bond length variations for both free LET and its complexed forms revealed that interactions along the direction of the triazole ring resulted in a reduction of bond lengths at the interaction sites. Conversely, other bond lengths exhibited minimal change. Approaching the drug toward rings containing nitrile groups and ethylene glycol segments led to an increase in certain bond lengths. An extensive examination of bond angles, as illustrated in Figures 2-a to 2-h, shows that during the approach of LET to the target molecules, the two six-membered rings bearing nitrile groups adopt conformations that favor enhanced interaction between the triazole ring and PLGA monomers. This orientation likely facilitates the drug's integration into the relatively bent structures of the PLGA components.

Comparison of bond angles among the selected complexes indicates that, in the LET-XXXY complex, where the C22–O65–C62 angle involves the triazole ring, the angle decreased from 117.03° to an average of 115.22°, implying that the two six-membered nitrile-containing rings are moving further apart to accommodate drug entry, bringing the drug closer to the molecular framework. Similarly, the C22–O66–C60 angle in the LET-XXYX complex decreased from 130.04° to an average of 115.92°, whereas in the LET-XYXX complex, it increased from 92.61° to 117.47°. Overall, the smaller variations observed in the bond angles of the LET-XXXY complex suggest a stabilization mechanism whereby, after encapsulation, individual monomers tend to fold inward, thereby aiding in the retention of the drug within the molecular structure.

3.2. Adsorption process and thermodynamic parameter

The capacity of PLGA monomers to adsorb the LET drug in various configurations was comprehensively investigated (Figure 2). To elucidate the nature of the adsorption process, thermodynamic parameters were calculated for the optimized complexes at a pressure of 1 atm and a temperature of 298 K. These parameters include the Gibbs free energy free energy change (ΔG) and enthalpy change (ΔH). The interaction energies and thermodynamic data are summarized in Tables 1 and 2, which detail the interaction processes of the complexes.

Based on the data presented in Table 1, the negative values of the adsorption energies (E_{ads}) confirm that the adsorption process occurs within thermodynamically stable configurations. Furthermore, the adsorption energy becomes more negative with an increasing number of monomers X and Y in the PLGA compositions.

Table 1. The values of absorption energy, enthalpy changes, and Gibbs free energy changes (in kcal/mol) for some complexes.

Systems	E_{ads}	ΔH	ΔG
LET-XY	-15.64	-12.36	-11.36
LET-XYYX	-19.73	-14.15	-13.28
LET-XYXX	-16.47	-11.49	-10.24
LET-XXYYY	-20.15	-11.15	-5.56
LET-(EG-XY-EG)	-24.33	-16.33	-12.98
LET-(XY-EG-XY)	-22.57	-20.58	-14.78
LET-(EG-XYXY-EG)	-39.12	-34.87	-30.15
LET-(EG-XYYX-EG)	-36.11	-30.21	-24.35
LET-(EG-XYXX-EG)	-38.71	-33.48	-29.17

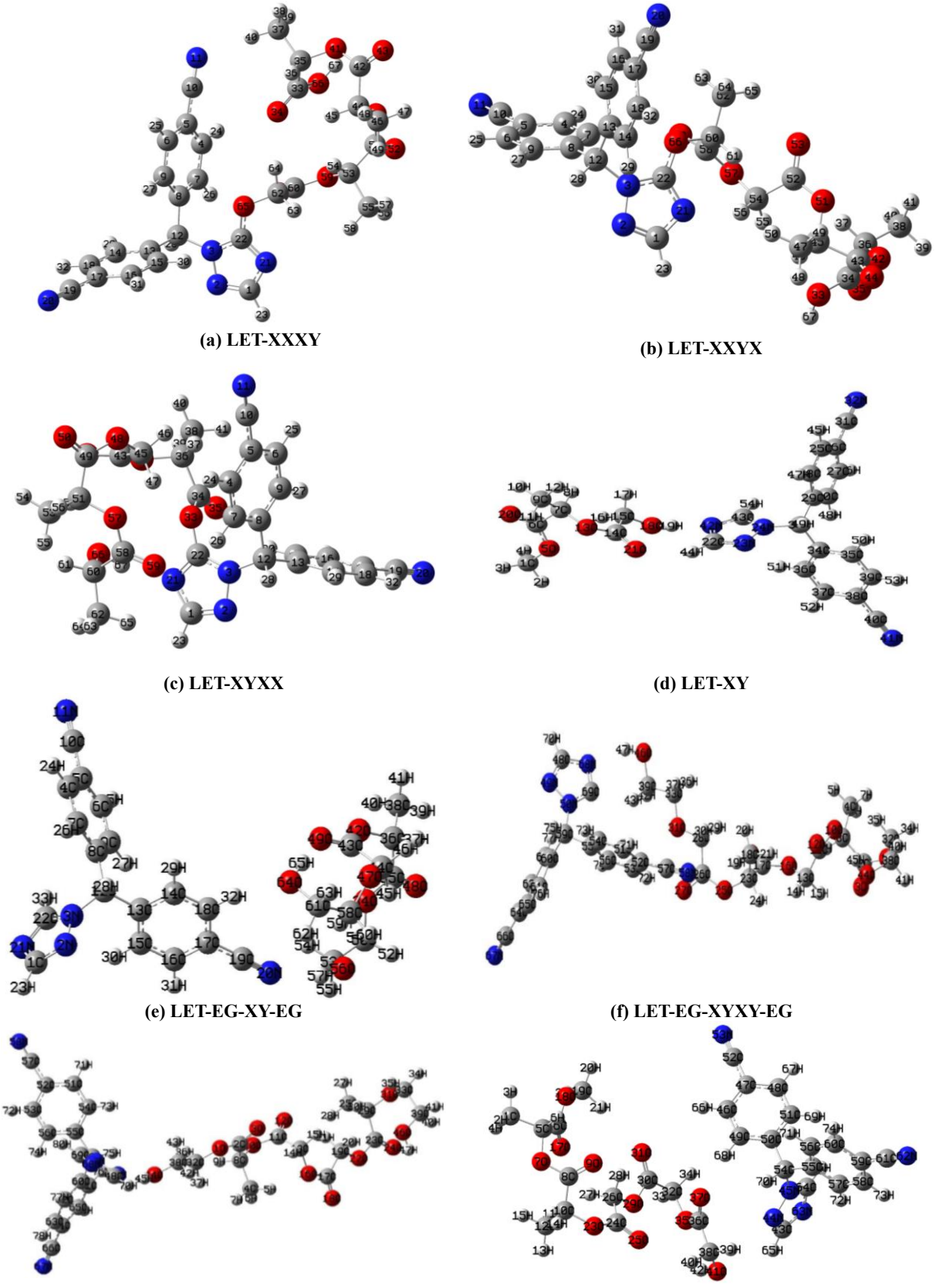

(a) LET-XXXY

(b) LET-XXYX

(c) LET-XYXX

(d) LET-XY

(e) LET-EG-XY-EG

(f) LET-EG-XYXY-EG

(g) LET- (EG-XYYX-EG)

(h) LET- XXYYY

Figure 2. Optimized geometric structure of compounds (a) LET-XXXY, (b) LET-XXYX, (c) LET-XYXX, (d) LET-XY, (e) LET-EG-XY-EG, (f) LET-EG-XYXY-EG, (g) LET-(EG-XYYX-EG), (h) LET-XXYYY.

The addition of EG to the PLGA monomers significantly enhances this effect, with the most substantial decrease observed when EG is attached at both ends. Additionally, the adsorption energy is influenced by the specific position of the monomers within the chain, indicating a dependence on monomer placement. The compounds XY and EG-XY-EG exhibit adsorption energies of -15.46 and -24.33 kcal/mol, respectively. In the XY complex, the interaction occurs primarily through the triazole ring, whereas in the EG-XY-EG complex, the interaction involves the six-membered ring containing the cyanide group. Notably, adsorption via the triazole ring results in a more negative energy, thereby contributing to a higher overall adsorption affinity of the complex. Among the studied complexes, the LET-(EG-XYXY-EG) complex exhibited the most negative interaction energy and the greatest adsorption affinity, with a value of -39.12 kcal/mol. As indicated by the negative ΔG values in Table 1, the adsorption process is spontaneous for all complexes. Moreover, the negative ΔH values suggest that the adsorption reactions are exothermic across the entire set of complexes. Consistent with the trend observed in the adsorption energies, the LET-(EG-XYXY-EG) complex displayed more negative thermodynamic parameters, reinforcing its higher stability.

Table 2. The values of absorption energy, enthalpy changes, and Gibbs free energy changes (in kcal/mol) for some complexes.

Systems	E_{ads}	ΔH	ΔG
LET-XY (Cyanide)	-30.11	-25.29	-25.18
LET-XXYX (Triazole)	-15.02	-10.18	-11.13
LET-XYXX (Triazole)	-16.71	-13.34	-13.00
LET-XXXY (Triazole)	-14.68	-10.31	-9.24
LET- XYXX (Cyanide)	-13.34	-9.54	-8.97

Based on the data presented in Table 2, the negative adsorption energies for all complexes indicate the thermodynamic stability of the interactions between the LET drug and the PLGA monomers. Furthermore, the negative values of ΔH and ΔG confirm that these interactions are exothermic and spontaneous. Notably, the LET-XY (Cyanide) complex exhibits the most negative adsorption energy and the most favorable thermodynamic properties among the studied complexes, suggesting that this interaction is the most thermodynamically preferred.

3.3. Electronic Parameters

The effect of the LET adsorption process on PLGA monomers was investigated using density functional theory calculations. Specifically, the energies of the highest occupied molecular orbital (HOMO) and the lowest unoccupied molecular orbital (LUMO) were computed before and after adsorption. The HOMO-LUMO energy gap (E_{gap}) was subsequently derived as the difference between LUMO and HOMO energies. The calculated values of E_{HOMO}, E_{LUMO}, E_{gap}, and E_F for complexes are summarized in Tables 3 and 4, respectively.

Table 3. The energy values of LUMO and HOMO, the energy gap (E_{gap}), and the Fermi level (E_F) of some complexes.

	E_{HOMO} (eV)	E_{LUMO} (eV)	E_{gap} (eV)	E_F (eV)
LET-XY	-6.92	-2.19	4.73	-4.55
LET-XYYX	-7.25	-1.91	5.34	-4.58
LET-XYXX	-7.18	-1.94	5.24	-4.56
LET-XXYYY	-7.19	-1.79	5.40	-4.49
LET-(EG-XY-EG)	-6.91	-0.02	4.89	-3.46
LET-(XY-EG-XY)	-6.97	-1.63	5.34	-4.3
LET-(EG-XYXY-EG)	-6.93	-2.54	4.39	-4.73
LET-(EG-XYYX-EG)	-6.76	-2.34	4.42	-4.55
LET-(EG-XYXX-EG)	-6.79	-1.72	5.07	-4.26

Analysis of the results presented in Tables 3 and 4 demonstrates that, across all examined cases, including the interaction of the drug LET with PLGA monomers and the conjugation of letrozole to PLGA via triazole rings and cyanide complexes, the resulting complexes exhibit a lower E_{gap} compared to their corresponding PLGA monomers. This indicates that these complexes possess higher reactivity. Furthermore, the incorporation of EG groups into the complexes further reduces the E_{gap}, thereby enhancing their reactivity. For example, the E_{gap} values for the structures LET-XYYX and LET-(EG-XYYX-EG) are 5.34 eV and 4.42 eV, respectively. Consequently, increasing the EG content correlates with an increase in the reactive propensity of these complexes.

Table 4. The energy values of LUMO and HOMO, the energy gap (E_{gap}), and the Fermi level (E_F) of some complexes.

	E_{HOMO} (eV)	E_{LUMO} (eV)	E_{gap} (eV)	E_F (eV)
LET-XY (Cyanide)	-5.52	-2.63	2.89	-4.08
LET-XXYX (Triazole)	-7.22	-1.94	5.28	-4.58
LET-XYXX (Triazole)	-7.30	-2.24	5.07	-4.77
LET-XXXY (Triazole)	-6.88	-1.80	5.08	-4.34
LET- XYXX (Cyanide)	7.03	-3.07	3.95	-5.05

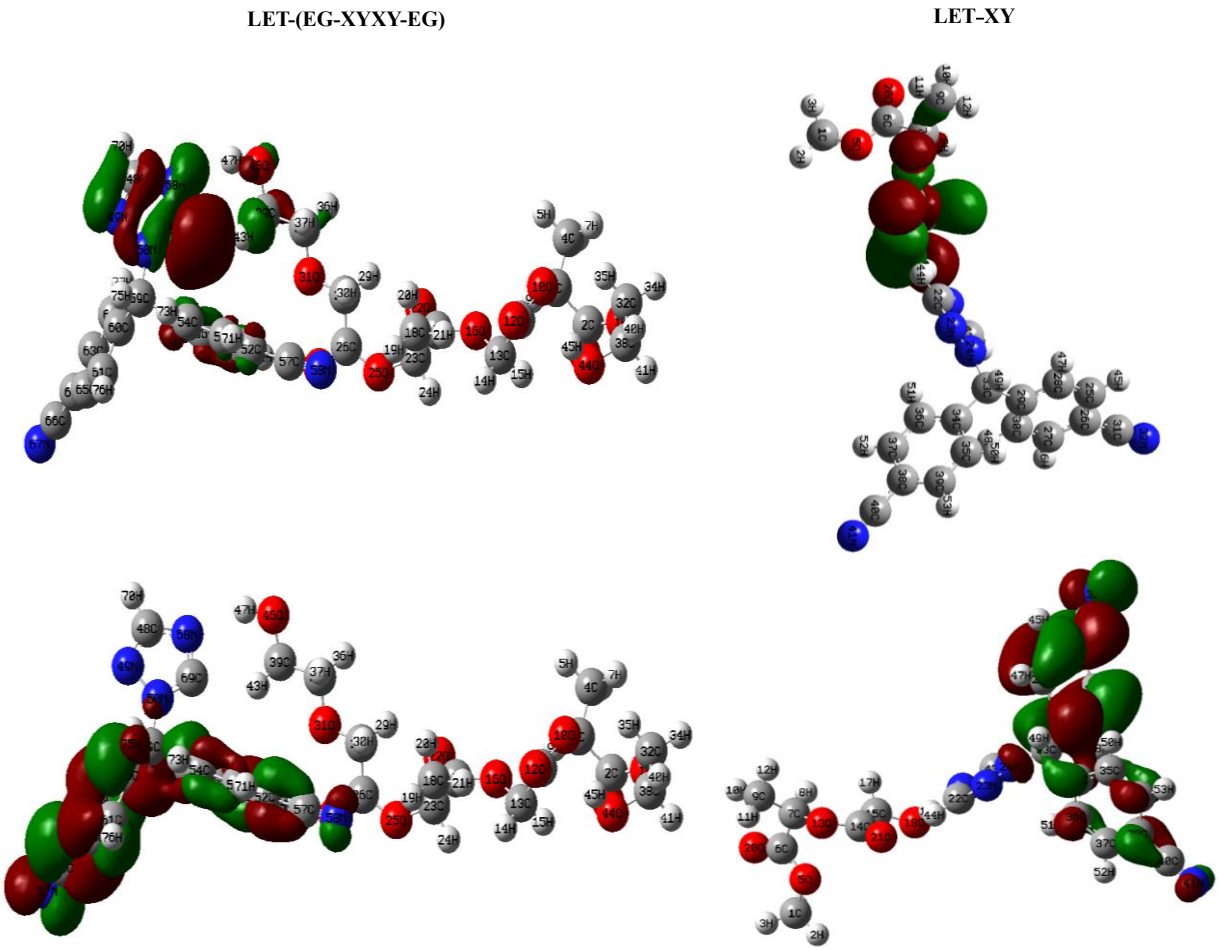

Figure 3. The orbital diagram of the LUMO and HOMO of the complexes LET-(EG-XYXY-EG).

The data presented in Table 4 demonstrate that the binding site of the drug on the PLGA monomers influences the E_{gap} values. Specifically, the complexes LET-XYXX (triazole) and LET-XYXX (cyanide) exhibit energy gap values of 5.07 eV and 3.95 eV, respectively. These findings suggest that the complex formed via the cyanide group of letrozole exhibits higher reactivity compared to that involving the triazole ring. Furthermore, when comparing these values to the complex resulting from non-specific interaction (no binding), which has an E_{gap} of 5.24 eV, it is evident that the bound complexes demonstrate increased reactivity. This indicates that binding induces electronic structural changes that enhance the chemical reactivity of the complexes. Figure 3 depicts the spatial distributions of HOMO and LUMO orbitals for the complexes.

The HOMO and LUMO orbital distributions for various complexes have been computed and analyzed, with the XY-LET complex exemplified in Figure 3. Analysis reveals that the majority of the LUMO density is localized on the six-membered ring of the letrozole molecule, which contains the cyanide group and a carbon atom with four different substituents. This localization can be attributed to the cyanide group, which tends to draw a significant electron density toward itself. The electron deficiency in the six-membered ring containing the cyanide group contributes to the concentration of the LUMO orbital in this region. Furthermore, Figure 3 indicates that the HOMO orbital is primarily localized on the hydroxyl and carbonyl groups at the termini of the PLGA monomers. The HOMO contribution is predominantly from these terminal groups. In some cases, the distribution extends to the triazole ring, with a higher density localized on the terminal groups compared to the triazole ring itself.

3.4. Global Indices of Reactivity

To comprehensively assess the impact of LET drug adsorption on PLGA monomers, the overall reactivity indices were calculated both prior to and following the adsorption process. Parameters such as ionization potential (IP), electron affinity (EA), chemical potential (μ), global hardness (η), global softness (S), electrophilicity index (ω), and

work function (Φ) were determined and summarized in Tables 5 and 6.

Table 5. Global reactivity indices values for some complexes.

	IP (eV)	**EA** (eV)	**μ**(eV)	**η** (eV)	**S**(eV)$^{-1}$	**ω** (eV)	**Φ** (eV)
LET-XY	6.92	2.19	-4.56	2.37	1.18	24.53	4.55
LET-XYYX	7.25	1.91	-4.58	2.67	1.34	28.00	4.58
LET-XYXX	7.18	1.94	-4.56	2.62	1.31	27.24	4.56
LET-XXYYY	7.19	1.79	-4.49	2.70	1.35	27.22	4.49
LET-(EG-XY-EG)	6.91	0.02	-3.47	3.45	1.72	20.68	3.46
LET-(XY-EG-XY)	6.97	1.63	-4.30	2.67	1.34	24.68	4.3
LET-(EG-XYXY-EG)	6.93	2.54	-4.74	2.20	1.10	24.61	4.73
LET-(EG-XYYX-EG)	6.76	2.34	-4.55	2.21	1.11	22.88	4.55
LET-(EG-XYXX-EG)	6.79	1.72	-4.26	2.5	1.27	22.95	4.25

Table 6. Global reactivity indices values for some complexes.

	IP (eV)	**EA** (eV)	**μ**(eV)	**η** (eV)	**S**(eV)$^{-1}$	**ω** (eV)	**Φ** (eV)
LET-XY (Cyanide)	5.52	2.63	-4.08	1.45	0.72	11.99	4.08
LET-XXYX (Triazole)	7.22	1.94	-4.58	2.64	1.32	27.69	4.58
LET-XYXX (Triazole)	7.3	2.24	-4.77	2.53	1.265	28.78	4.77
LET-XXXY (Triazole)	6.88	1.8	-4.34	2.54	1.27	23.92	4.34
LET- XYXX (Cyanide)	7.03	3.07	-5.05	1.98	0.99	25.25	5.05

The data in Table 4 demonstrate that increasing the proportion of ethylene glycol (EG) in the PLGA monomers results in a reduction of the chemical hardness of the formed complex. This observation is supported by the comparison of the LET-XYYX and LET-(EG-XYYX-EG) compounds, which exhibit chemical hardness values of 2.67 eV and 2.21 eV, respectively, as well as by the comparison between LET-XYYX and LET-(EG-XYXX-EG), with values of 2.67 eV and 2.54 eV, respectively. Further analysis of the data indicates that the chemical hardness of the letrozole–PLGA complex is consistently lower than that of the corresponding PLGA derivatives in both EG-present and EG-absent states. Additionally, the chemical potential and nucleophilicity index of the resulting complexes are higher across all cases for the PLGA-based compounds.

Based on the data presented in Table 6, it is evident that chemical hardness decreases upon bonding the drug and compounds from all interaction sites. Notably, compounds containing a cyanide group attached to the aromatic ring exhibit a more pronounced reduction in chemical hardness, suggesting that bonds involving the cyanide group are more reactive. Further analysis indicates that, in all cases, attachment via the cyanide group or the triazole ring results in complexes with lower chemical hardness and increased chemical potential and nucleophilicity indices compared to the corresponding PLGA derivatives.

3.5. Dipole Moment (μ) Analysis

Polarity is a fundamental characteristic of chemical bonds. When two atoms involved in a covalent bond have different electronegativities, the bonding electrons are drawn unevenly, following the principle of electronegativity disparity. This results in a separation of positive and negative charge centers within the bond, rendering it an electric dipole thus, it is classified as a polar bond. In molecules with multiple atoms, overall polarity is assessed by the resulting dipole moment, which determines whether the molecule exhibits polar or nonpolar behavior. Variations in the dipole moment can also provide insights into the drug's solubility and its release behavior at the intended target. The dipole moment values, measured in Debye units for the complexes, have been calculated and are presented in the graphs of Figures 4 and 5.

The values of the electric dipole moment, as reported in Figure 4, demonstrate that increasing the concentration of both monomers, Y

and X, in the letrozole–PLGA complexes results in a corresponding rise in dipole moment. Furthermore, the dipole moment of the complexes is influenced by the position of the monomers within the PLGA backbone. Notably, the attachment of ethylene glycol (EG) role than the cyanide group. This is likely due to the greater polarity of the nitrogen atoms in the triazole ring, stemming from their sp^2 hybridization, in contrast to the sp hybridization of nitrogen in the cyanide group. The higher polarity of the nitrogen in the triazole ring

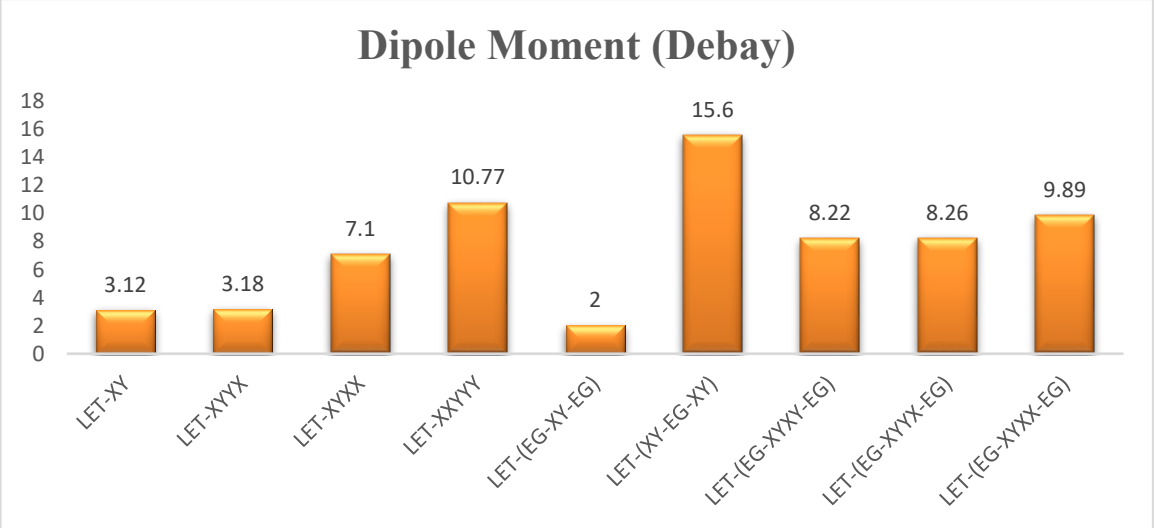

Fig4. The plot of the dipole moment values of some complexes in Debye.

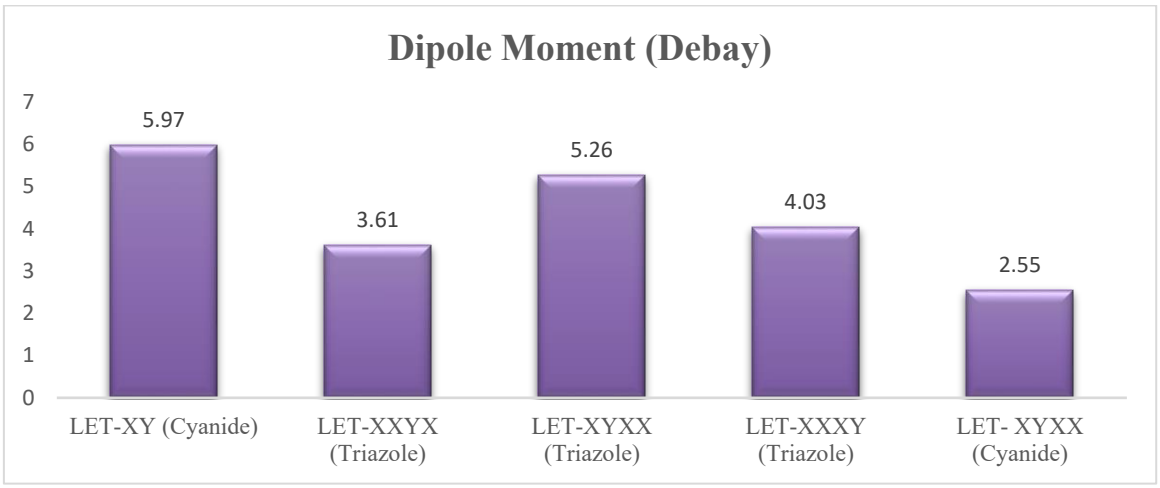

Figure 5. The plot of the dipole moment values of some complexes in Debye.

markedly enhances the dipole moment; for instance, the dipole moment of LET-(XYYX) increases from 3.18 Debye in LET-(EG-XYYX-EG) to 8.26 Debye.

Analysis of the results presented in Figure 5 indicates that the dipole moments of LET-XYXX (triazole) and LET-(XYXX) (cyanide group) are 4.03 Debye and 2.55 Debye, respectively. This suggests that the dipole moment of the resulting complex formed through the interaction of letrozole with PLGA compounds is higher when bonding occurs via the triazole ring compared to the cyanide group attached to the six-membered ring. It can be inferred that this difference reflects a preferred interaction pathway for letrozole, with the three nitrogen atoms in the triazole ring playing a more prominent enhances its tendency to participate in interactions.

4. Conclusions

This study investigates the structural, electronic, and thermodynamic properties of PLGA complexes with the anticancer drug letrozole. The formation of the complex causes significant changes in bond lengths and angles, especially at the reactive site where the drug approaches the compounds. Despite the large size of the molecules, these alterations are notable and depend on the approach direction of the drug. When the drug approaches the five-membered nitrogen-containing triazole ring, the bond lengths decrease, whereas approaching from the N-part of the cyanide group attached to a six-membered ring results in increased bond lengths. The nitrogen atom

in the triazole ring that interacts with the terminal OH group in the compounds tends to attract electrons due to its electronegativity, drawing electron density toward the complex. The five-membered ring's three nitrogen atoms, rich in electron pairs, are considered part of the HOMO. If the carbonyl group is terminal, it tends to donate electrons, while oxygen in the OH group attracts electrons more strongly when present at the end of the molecule. Furthermore, the complex formation causes the triazole ring to bend more easily into the cavity of the compounds compared to the other rings, ensuring the drug is effectively encapsulated. An observed decrease in the angle between the drug and the compounds correlates with shorter bond lengths in this region, with minimal changes elsewhere. The polarity of the LET-XXYX complex surpasses that of the LET-XXXY complex, primarily due to higher symmetry in the XXYX structure. This increased symmetry results from differences in how the terminal OH groups are attached: in monomer X, the OH attaches to a carbon with a methyl group, whereas in monomer Y, it attaches to a carbon bonded to two hydrogens. The more symmetrical structure in Y enhances the overall dipole moment. Additionally, adding ethylene glycol groups to the ends of PLGA decreases chemical hardness while increasing chemical potential and electronegativity. It also raises absorption and reactivity energies, indicating that such modifications could improve the complex's stability and reactivity. These findings suggest a promising strategy for targeted drug delivery of letrozole, offering potential improvements for therapeutic applications.

Acknowledgements

We acknowledge the University of Mazandaran for financial support of this work.

Conflicts of interest/Competing interests: The authors declare that they have no conflict of interest and no competing interests exist.

Ethics approval: The manuscript is prepared in compliance with the Ethics in Publishing Policy as described in the Guide for Authors.

Funding Declaration: This research received no external funding.

Consent to participate: The manuscript is approved by all authors for publication.

Consent for publication: The consent for publication was obtained formal participants.

References

[1] Siddiqa, A.J., Chaudhury, K., Adhikari, B. Letrozole dispersed on poly (vinyl alcohol) anchored maleic anhydride grafted low density polyethylene: A controlled drug delivery system for treatment of breast cancer. *Colloids and Surfaces B: Biointerfaces*. **2014**, 116, 169-75.

[2] Bowman, A., Gabra, H., Langdon, S.P., Lessells, A., Stewart, M., Young, A., et al. CA125 response is associated with estrogen receptor expression in a phase II trial of letrozole in ovarian cancer: identification of an endocrine-sensitive subgroup. *Clinical cancer research*. **2002**, 8, 2233-9.

[3] Castonguay, A., Doucet, C.d., Juhas, M., Maysinger, D. New ruthenium (II)–letrozole complexes as anticancer therapeutics. *Journal of Medicinal Chemistry*. **2012**, 55, 8799-806.

[4] Haynes, B., Dowsett, M., Miller, W., Dixon, J., Bhatnagar, A. The pharmacology of letrozole. *The Journal of steroid biochemistry and molecular biology*. **2003**, 87, 35-45.

[5] Mlaouah, M., Tangour, B., El Khalifi, M., Gharbi, T., Picaud, F. The encapsulation of the gemcitabine anticancer drug into grapheme nest: a theoretical study. *Journal of Molecular Modeling*. **2018**, 24, 1-9.

[6] Aminu, N., Bello, I., Umar, N.M., Tanko, N., Aminu, A., Audu, M.M. The influence of nanoparticulate drug delivery systems in drug therapy. *Journal of drug delivery science and technology*. **2020**, 60, 101961.

[7] Rezvantalab, S., Moraveji, M.K., Khedri, M., Maleki, R. An insight into the role of riboflavin ligand in the self-assembly of poly (lactic-co-glycolic acid)-based nanoparticles–a molecular simulation and experimental approach. *Soft Matter*. **2020**, 16, 5250-60.

[8] Oh, J.K. Polylactide (PLA)-based amphiphilic block copolymers: synthesis, self-assembly, and biomedical applications. *Soft Matter*. **2011**, 7, 5096-108.

[9] Lü, J.-M., Wang, X., Marin-Muller, C., Wang, H., Lin, P.H., Yao, Q., et al. Current advances in research and clinical applications of PLGA-based nanotechnology. *Expert review of molecular diagnostics*. **2009**, 9, 325-41.

[10] Locatelli, E., Comes Franchini, M. Biodegradable PLGA-b-PEG polymeric nanoparticles: synthesis, properties, and nanomedical applications as drug delivery system. *Journal of Nanoparticle Research*. **2012**, 14, 1-17.

[11] Bogdanova, S., Pajeva, I., Nikolova, P., Tsakovska, I., Müller, B. Interactions of poly (vinylpyrrolidone) with ibuprofen and naproxen: Experimental and modeling studies. *Pharmaceutical research*. **2005**, 22, 806-15.

[12] Jeong, B., Bae, Y.H., Kim, S.W. Thermoreversible gelation of PEG− PLGA− PEG triblock copolymer aqueous solutions. *Macromolecules*. **1999**, 32, 7064-9.

[13] Ghahremankhani, A.A., Dorkoosh, F., Dinarvand, R. PLGA-PEG-PLGA tri-block copolymers as in situ gel-forming peptide delivery system: effect of formulation properties on peptide

release. *Pharmaceutical development and technology*. **2008**, 13, 49-55.

[14] Makadia, H.K., Siegel, S.J. Poly lactic-co-glycolic acid (PLGA) as biodegradable controlled drug delivery carrier. *Polymers*. **2011**, 3, 1377-97.

[15] Akçay, H.T., Bayrak, R. Computational studies on the anastrozole and letrozole, effective chemotherapy drugs against breast cancer. *Spectrochimica Acta Part A: Molecular and Biomolecular Spectroscopy*. **2014**, 122, 142-52.

[16] Becke, A.D. Density-functional thermochemistry. I. The effect of the exchange-only gradient correction. *The Journal of chemical physics*. **1992**, 96, 2155-60.

[17] Ghasemi, A., Taghartapeh, M.R., Soltani, A., Mahon, P.J. Adsorption behavior of metformin drug on boron nitride fullerenes: Thermodynamics and DFT studies. *Journal of Molecular Liquids*. **2019**, 275, 955-67.

[18] Lipin, R., Dhanabalan, A.K., Gunasekaran, K., Solomon, R.V. Piperazine-substituted derivatives of favipiravir for Nipah virus inhibition: What do in silico studies unravel? *SN Applied Sciences*. **2021**, 3, 110.

[19] Yuksel, N., Köse, A., Fellah, M.F. The supramolecularly complexes of calix [4] arene derivatives toward favipiravir antiviral drug (used to treatment of COVID-19): a DFT study on the geometry optimization, electronic structure and infrared spectroscopy of adsorption and sensing. *Journal of Inclusion Phenomena and Macrocyclic Chemistry*. **2021**, 101, 77-89.

[20] Ibrahim, M.A., Shehata, M.N., Moussa, N.A., Hemia, R.R., Abd Elhafez, H.S., Abd El-Rahman, M.K., et al. Preferability of Molnupiravir, an anti-COVID-19 drug, toward purine nucleosides: A quantum mechanical study. *ACS omega*. **2023**, 8, 27553-65.

[21] Frisch, M. gaussian 09, Revision d. 01, Gaussian. *Inc, Wallingford CT*. **2009**, 201.